

Improved polygenic prediction by Bayesian multiple regression on summary statistics

Luke R. Lloyd-Jones^{1, **}, Jian Zeng^{1, **}, Julia Sidorenko^{1,4}, Loïc Yengo¹, Gerhard Moser^{3,4}, Kathryn E. Kemper¹, Huanwei Wang¹, Zhili Zheng¹, Reedik Magi^{4,5}, Tonu Esko^{4,5}, Andres Metspalu^{4,5}, Naomi R. Wray^{1,2}, Michael E. Goddard³, Jian Yang^{1, 2} and Peter M. Visscher^{1, 2}

¹Institute for Molecular Bioscience, University of Queensland, Brisbane, Queensland 4072, Australia, ²Queensland Brain Institute, University of Queensland, Brisbane, Queensland 4072, Australia, ³School of Engineering and Technology, Central Queensland University, Rockhampton, 4702, Queensland, Australia, ⁴Australian Agricultural Company Ltd, Brisbane, 4006, Queensland, Australia, ⁵Faculty of Veterinary and Agricultural Science, University of Melbourne, 3052 Victoria, Australia, ⁶Estonian Genome Center, University of Tartu, Tartu, Estonia, ⁷Institute of Molecular and Cell Biology, University of Tartu, Tartu, Estonia, ^{**}These two authors contributed equally.

ABSTRACT The capacity to accurately predict an individual's phenotype from their DNA sequence is one of the great promises of genomics and precision medicine. Recently, Bayesian methods for generating polygenic predictors have been successfully applied in human genomics but require the individual level data, which are often limited in their access due to privacy or logistical concerns, and are computationally very intensive. This has motivated methodological frameworks that utilise publicly available genome-wide association studies (GWAS) summary data, which now for some traits include results from greater than a million individuals. In this study, we extend the established summary statistics methodological framework to include a class of point-normal mixture prior Bayesian regression models, which have been shown to generate optimal genetic predictions and can perform heritability estimation, variant mapping and estimate the distribution of the genetic effects. In a wide range of simulations and cross-validation using 10 real quantitative traits and 1.1 million variants on 350,000 individuals from the UK Biobank (UKB), we establish that our summary based method, SBayesR, performs similarly to methods that use the individual level data and outperforms other state-of-the-art summary statistics methods in terms of prediction accuracy and heritability estimation at a fraction of the computational resources. We generate polygenic predictors for body mass index and height in two independent data sets and show that by exploiting summary statistics on 1.1 million variants from the largest GWAS meta-analysis ($n \approx 700,000$) that the SBayesR prediction R^2 improved on average across traits by 6.8% relative to that estimated from an individual-level data BayesR analysis of data from the UKB ($n \approx 450,000$). Compared with commonly used state-of-the-art summary-based methods, SBayesR improved the prediction R^2 by 4.1% relative to LDpred and by 28.7% relative to clumping and p -value thresholding. SBayesR gave comparable prediction accuracy to the recent RSS method, which has a similar model, but at a computational time that is two orders of magnitude smaller. The methodology is implemented in a very efficient and user-friendly software tool titled GCTB.

KEYWORDS Complex trait genetics; Genome-wide association studies; Linear mixed models; UK Biobank; High-dimensional regression

1 Introduction

2 The capacity to accurately predict an individual's phenotype from their DNA sequence
3 is one of the great promises of genomics and precision medicine^{1–5}, recognising that the
4 accuracy of a genetic risk predictor is dependent on the genetic contribution to variation
5 in the trait. It is anticipated that genetic risk prediction will be useful for informing early
6 disease intervention and aiding diagnosis by identifying individuals with an increased
7 genetic risk of disease^{5–7}. Accurate genetic predictors for complex traits and disorders are
8 currently limited, due mainly to an incomplete understanding of complex genetic varia-
9 tion, small training sample sizes and suboptimal modelling^{4,8,9}. Through large consortia
10 and biobank initiatives, sample sizes for genome-wide association studies (GWASs) are
11 reaching a critical point, now for some traits greater than a million individuals, at which,
12 and under optimal modelling conditions, the predictors generated could approach their
13 maximum (from theory) prediction accuracy for some traits^{10–13}.

14 One common approach for generating polygenic predictions uses GWASs effect size
15 estimates derived from simple linear regression applied to each single-nucleotide poly-
16 morphism (SNP) independently across the genome, and uses a linear combination of the
17 estimated effects and allele counts at genetic markers, chosen via marker pruning coupled
18 with *p*-value thresholding^{14–17}. Although simple to implement and useful, this method
19 has been shown to provide suboptimal predictions with the best estimate of each marker's
20 effect requiring the effects to be treated as random^{18–20}. In this work, we will restrict the
21 term polygenic risk score to those predictors generated from using simple linear regression
22 and use the term estimated genetic value (EGV) for the general concept of generating a
23 polygenic predictor from SNP data. Linear mixed model (LMM) methodologies have been
24 successfully applied in human genetics^{21–25} and are derived under the multiple regression
25 model. These methods jointly analyse all SNPs, which accounts for linkage disequilibrium
26 (LD) between markers capturing the maximum amount of variation at a genetic locus
27 especially if multiple causal variants colocalise. Bayesian extensions of the standard LMM,
28 which assumes a single normal distribution on the genetic effects, have been made to

29 include alternative prior distributions for the genetic effects that deviate from the assumptions of the infinitesimal model, and were pioneered in plant and animal breeding²⁶⁻³⁰.

30 Recent implementations of Bayesian multiple regression methodology require access to the individual level data^{29,31} and currently do not scale well computationally to sample sizes of greater than half a million individuals and millions of genetic variants.

31 The inability to access individual level genetic and phenotypic data has motivated methodological frameworks that only require publicly available summary data⁹. Summary statistics methodology now covers the gamut of statistical genetics analyses including: effect size distribution estimation^{32,33}, joint SNP association analysis and fine mapping^{34,35}, allele frequency and association statistic imputation³⁶⁻³⁸, heritability and genetic correlation estimation³⁹⁻⁴³ and polygenic prediction⁴⁴⁻⁴⁶. These methods require GWAS summary data, which typically include the estimated univariate effect, standard error, sample size and allele frequency, and an estimate of LD among genetic markers, which are easily accessed via public databases.

32 In this work, we extend the established summary statistics methodological framework through the utilisation of a likelihood that connects the multiple regression coefficients with the summary statistics from GWAS (similar to Zhu and Stephens⁴²). We perform Bayesian posterior inference through the combination of this likelihood and a finite mixture of normal distributions prior on the markers effects, which encompasses the models proposed in Habier *et al.*²⁷, Erbe *et al.*²⁸ and Moser *et al.*³¹. Here, we focus on optimising prediction accuracy but the methodology is capable of simultaneously estimating SNP-based heritability (h_{SNP}^2), marker mapping and estimating the distribution of marker effects. We maximise computational efficiency by taking advantage of LD matrix sparsity and, importantly, once the GWAS effect size estimates have been generated the computational time of our method is independent of sample size making the method applicable to an arbitrary number of individuals.

33 We establish that our summary-based method, SBayesR, outperforms other state-of-the-art summary statistics methods in terms of prediction accuracy and h_{SNP}^2 estimation in a

57 wide range of simulations using real genotype data from 350,000 unrelated individuals of
58 European ancestry from the UK Biobank (UKB). The state-of-the-art summary statistics
59 methods used for comparison include those that seek to estimate posterior mean effect
60 sizes from GWAS summary statistics by assuming a prior for the genetics effects and
61 LD information from a reference panel stored for each chromosome in a block diagonal
62 form or constructed from an LD matrix shrinkage estimator. Specifically, we compare
63 with LDpred⁴⁴, which assumes a point-normal mixture prior for the genetics effects and a
64 block-diagonal LD matrix, summary best linear unbiased prediction (SBLUP)⁴⁵, which
65 assumes a normal distribution for the genetics effects and a block-diagonal LD matrix,
66 Regression with Summary Statistics (RSS)⁴², which has a class of priors for the genetic
67 effects to select from but we compare against the mixture of two normal distributions
68 prior²⁹ and is optimised for the use of a shrunk LD matrix³⁶. We further compare with
69 clumping and then *p*-value thresholding (P+T) implemented in the PLINK 2 software⁴⁷
70 and the individual data implementation of the BayesR model³¹, which assumes a finite
71 mixture of normal distributions (including a point mass at zero) prior on the genetic effects
72 and has been optimised for time and memory efficiency. For h_{SNP}^2 estimation comparison
73 we use the widely used summary data LD score regression (LDSC) method³⁹, which relies
74 on the expected relationship between, under a polygenic model, per variant chi-squared
75 summary statistics and LD scores from a reference, RSS, which can estimate h_{SNP}^2 given the
76 posterior mean of the genetics effects and the individual data Haseman-Elston regression
77 (HReg) method⁴⁸, which relies on identity by state relatedness measures derived from a
78 genetic relatedness matrix and the cross product of the phenotypes for pairwise individuals
79 and is efficient on large data sets.

80 We show that SBayesR performs similarly in terms of prediction accuracy to individual
81 data methods and outperforms other state-of-the-art summary methods in five-fold cross-
82 validation with 1.1 million HapMap 3 (HM3) variants and 10 real quantitative traits
83 from the UKB. We further perform large-scale analyses for height and body mass index
84 using 1.1 million HM3 variants and the full UKB European ancestry (both related and

85 unrelated individuals) data set and predict into two independent samples from the Health
86 and Retirement Study (HRS) and the Estonian Biobank (ESTB). In these across biobank
87 analyses, we show that by exploiting summary statistics from the largest GWAS meta-
88 analysis ($n \approx 700,000$) on height and body mass index⁴⁹ that on average across traits
89 the SBayesR prediction accuracy improved by 6.8% relative to that estimated from an
90 individual-level data BayesR analysis of data from the UKB ($n \approx 450,000$). Compared
91 with commonly used state-of-the-art summary-based methods, SBayesR improved the
92 prediction R^2 by 4.1% relative to LDpred and by 28.7% relative to clumping and p -value
93 thresholding. SBayesR gave comparable prediction accuracy to the recent RSS method,
94 which has a similar algorithm, but at a computational time that is two orders of magnitude
95 smaller. The methodology is implemented in a very efficient and user-friendly software
96 tool titled GCTB³⁰.

97 Materials and Methods

98 Data

99 **UK Biobank** We used real genotype and phenotype data from the full release of the UK
100 Biobank (UKB). The UKB is a prospective community cohort of over 500,000 individu-
101 als from across the United Kingdom and contains extensive phenotypic and genotypic
102 information about its participants⁵⁰. The UKB data contains genotypes for 488,377 in-
103 dividuals (including related individuals) that passed sample quality control (99.9% of
104 total samples). A subset of 456,426 European ancestry individuals was selected using the
105 protocol described in Yengo *et al.*⁴⁹. To exclude related individuals, a genomic relationship
106 matrix (GRM) was constructed with 1,123,943 HM3 variants further filtered for minor allele
107 frequency (MAF) > 0.01 , pHWE $< 10^{-6}$ and missingness < 0.05 in the European subset,
108 resulting in a final set of 348,580 unrelated (absolute GRM off-diagonal < 0.05) Europeans.
109 Genotype data were imputed to the Haplotype reference consortium and UK10K panel,
110 which was provided as part of the data release and described in⁵⁰, and contained SNPs,
111 short indels and large structural variants. Variant quality control included: removal of

112 multi-allelic variants, SNPs with imputation info score < 0.3, retained SNPs with hard-call
113 genotypes with > 0.9 probability, removed variants with minor allele count (MAC) ≤ 5 ,
114 Hardy-Weinberg *p*-value (pHWE) $< 10^{-5}$ and removed variants with missingness > 0.05,
115 which resulted in 46,500,935 SNPs for the 456,426 individuals.

116 ***Atherosclerosis Risk in Communities, 1000 Genomes and UK10K data*** The implemented
117 summary statistics methodology requires an estimate of LD among genetic markers. In
118 addition to the UKB, three data sets were used to calculate LD reference matrices. We
119 used the genotype data from the Atherosclerosis Risk in Communities (ARIC)⁵¹ and
120 GENEVA Diabetes study obtained via dbGaP. The ARIC+GENEVA data consisted of
121 12,942 unrelated individuals determined by an absolute GRM off-diagonal relatedness
122 cutoff of < 0.05. After imputation to the Phase 3 of the 1000 Genomes Project (1000G)⁵²,
123 1,182,558 HM3 SNPs (MAF > 0.01) were selected and available for analysis after quality
124 control. Whole-genome sequencing data from the 1000G project was used for LD matrix
125 reference calculation. These data were subsetted to a set of 397 individuals with European
126 ancestry to be consistent with the LD reference used in Zhu and Stephens⁴². Whole-
127 genome sequencing data from the UK10K project⁵³ was also used for analysis. The UK10K
128 contains 17.6 million genetic variants (excluding singletons and doubletons) in 3,642
129 unrelated individuals after quality control, which was performed as per Yang *et al.*⁵⁴.

130 ***Health and Retirement Study and Estonian Biobank*** For out-of-sample validation of ge-
131 netic predictors we used two cohorts that are independent of the UKB. We used genotypes
132 imputed to the 1000G reference panel and phenotypes from 8,552 unrelated (absolute
133 GRM off-diagonal < 0.05) participants of the Health and Retirement Study (HRS)⁵⁵. After
134 imputation and restricting variants with an imputation quality score > 0.3, MAF > 0.01
135 and a pHWE $> 10^{-6}$ there were 24,777,992 SNPs available for prediction. The Estonian
136 Biobank⁵⁶ is a cohort study of over 50,000 individuals over 18 years of age with phenotypic
137 and genotypic data. For the prediction analysis we used data from 32,594 individuals
138 genotyped on the Global Screening Array. These data were imputed to the Estonian
139 reference⁵⁷, created from the whole genome sequence data of 2,244 participants. Markers

¹⁴⁰ with imputation quality score > 0.3 were selected leaving a total of 11,130,313 SNPs for
¹⁴¹ prediction.

¹⁴² ***Overview of summary statistics based Bayesian multiple regression***

¹⁴³ We relate the phenotype to the set of genetic variants under the multiple linear regression
¹⁴⁴ model

$$\mathbf{y} = \mathbf{X}\boldsymbol{\beta} + \boldsymbol{\varepsilon}, \quad (1)$$

¹⁴⁵ where \mathbf{y} is an $n \times 1$ vector of trait phenotypes, which has been centred, \mathbf{X} is an $n \times p$ matrix
¹⁴⁶ of genotypes coded as 0, 1 or 2 representing the number of copies of the reference allele at
¹⁴⁷ each marker, $\boldsymbol{\beta}$ is a $p \times 1$ vector of multiple regression coefficients (marker effects) and $\boldsymbol{\varepsilon}$ is
¹⁴⁸ the error term ($n \times 1$). We can relate the multiple regression model to the estimates of the
¹⁴⁹ regression coefficients from p simple linear regressions \mathbf{b} from GWAS, by multiplying (1)
¹⁵⁰ by $\mathbf{D}^{-1}\mathbf{X}'$ where $\mathbf{D} = \text{diag}(\mathbf{x}_1' \mathbf{x}_1, \dots, \mathbf{x}_p' \mathbf{x}_p)$ to arrive at

$$\mathbf{D}^{-1}\mathbf{X}'\mathbf{y} = \mathbf{D}^{-1}\mathbf{X}'\mathbf{X}\boldsymbol{\beta} + \mathbf{D}^{-1}\mathbf{X}'\boldsymbol{\varepsilon}. \quad (2)$$

Noting that $\mathbf{b} = \mathbf{D}^{-1}\mathbf{X}'\mathbf{y}$ is the vector ($p \times 1$) of least-squares marginal regression effect
estimates and the correlation matrix between all genetic markers $\mathbf{B} = \mathbf{D}^{-\frac{1}{2}}\mathbf{X}'\mathbf{X}\mathbf{D}^{-\frac{1}{2}}$, we
¹⁵¹ rewrite the multiple regression model as

$$\mathbf{b} = \mathbf{D}^{-\frac{1}{2}}\mathbf{B}\mathbf{D}^{\frac{1}{2}}\boldsymbol{\beta} + \mathbf{D}^{-1}\mathbf{X}'\boldsymbol{\varepsilon}. \quad (3)$$

Assuming $\boldsymbol{\varepsilon}_1, \dots, \boldsymbol{\varepsilon}_n$ are independent $N(0, \sigma_\varepsilon^2)$, the following likelihood can be proposed
¹⁵² for the multiple regression coefficients $\boldsymbol{\beta}$

$$\mathcal{L}(\boldsymbol{\beta}; \mathbf{b}, \mathbf{D}, \mathbf{B}) := \mathcal{N}(\mathbf{b}; \mathbf{D}^{-\frac{1}{2}}\mathbf{B}\mathbf{D}^{\frac{1}{2}}\boldsymbol{\beta}, \mathbf{D}^{-\frac{1}{2}}\mathbf{B}\mathbf{D}^{-\frac{1}{2}}), \quad (4)$$

153 where $\mathcal{N}(\boldsymbol{\xi}; \boldsymbol{\mu}, \boldsymbol{\Sigma})$ represents the multivariate normal distribution with mean vector $\boldsymbol{\mu}$ and
 154 covariance matrix $\boldsymbol{\Sigma}$ for $\boldsymbol{\xi}$. If individual level data are available then inference about $\boldsymbol{\beta}$ can
 155 be obtained by replacing \mathbf{D} and \mathbf{B} with estimates $(\widehat{\mathbf{D}}, \widehat{\mathbf{B}})$ from the individual level data. If
 156 individual level data are unavailable then we can replace \mathbf{D} with $\widehat{\mathbf{D}} = \text{diag}\{1/[\widehat{\sigma}^2(b_1) +$
 157 $b_1^2/n_1], \dots, 1/[\widehat{\sigma}^2(b_p) + b_p^2/n_p]\}$, where $[n_j, b_j, \widehat{\sigma}^2(b_j)]$ are the sample size used to compute
 158 the simple linear regression coefficient, an estimate of the simple linear regression allele
 159 effect coefficient and $\widehat{\sigma}(b_j)$ the standard error of the effect for the j th variant respectively.
 160 This reconstruction of $\widehat{\mathbf{D}}$ assumes that the markers have been centred to mean 0 (please see
 161 the Supplemental Note for a detailed reasoning of this reconstruction of $\widehat{\mathbf{D}}$). If we make
 162 the further assumption that the genetic markers have been scaled to unit variance then
 163 we can replace \mathbf{D} with $\widehat{\mathbf{D}} = \text{diag}\{n_1, \dots, n_p\}$. Similarly, we replace \mathbf{B} , the LD correlation
 164 matrix between the genotypes at all markers in the population, which the genotypes in
 165 the sample are assumed to be a random sample, with $\widehat{\mathbf{B}}$ an estimate calculated from a
 166 population reference that is assumed to closely resemble the sample used to generate the
 167 GWAS summary statistics. Zhu and Stephens⁴² discuss further the theoretical properties of
 168 a similar likelihood. We assess the limits of replacing \mathbf{D} and \mathbf{B} with these approximations
 169 through simulation and real data analysis.

170 We perform Bayesian posterior inference by assuming a prior on the multiple regression
 171 genetic effects and the posterior

$$p(\boldsymbol{\beta}|\mathbf{b}, \mathbf{D}, \mathbf{B}) \propto p(\mathbf{b}|\boldsymbol{\beta}, \mathbf{D}, \mathbf{B})p(\boldsymbol{\beta}|\mathbf{D}, \mathbf{B}). \quad (5)$$

172 In this paper we implement the BayesR model^{28,31}, which assumes that

$$\beta_j | \boldsymbol{\pi}, \sigma_{\beta}^2 = \begin{cases} 0 & \text{with probability } \pi_1, \\ \sim N(0, \gamma_2 \sigma_{\beta}^2) & \text{with probability } \pi_2, \\ \vdots \\ \sim N(0, \gamma_C \sigma_{\beta}^2) & \text{with probability } 1 - \sum_{c=1}^{C-1} \pi_c, \end{cases}$$

173 where C denotes the maximum number of components in the finite mixture model, which
 174 is prespecified. The γ_c coefficients are prespecified and constrain how the common marker
 175 effect variance σ_β^2 scales in each distribution. In previous implementations of BayesR
 176 the variance weights γ were with respect to the genetic variance σ_g^2 . For example, it
 177 is common in the BayesR model to assume $C = 4$ such that $\gamma = (\gamma_1, \gamma_2, \gamma_3, \gamma_4)' =$
 178 $(0, 0.0001, 0.001, 0.01)'$. This requires the genotypes to be centred and scaled and equates
 179 $\sigma_g^2 = m\sigma_\beta^2$, where m is the number of variants. We relax this assumption to disentangle
 180 the relationship between these parameters and to maintain the flexibility of the model
 181 to assume scaled or unscaled genotypes. In this implementation, we let the weights
 182 be with respect to σ_β^2 and have a default $\gamma = (0, 0.01, 0.1, 1.0)'$, which maintains the
 183 relative magnitude of the variance classes as in the original model. The Supplementary
 184 Note details further the hierarchical model and hyperparameter prior specification. The
 185 Supplementary Note also details the derivation of the Markov chain Monte Carlo Gibbs
 186 sampling routine for sampling of the key model parameters $\theta = (\beta', \pi', \sigma_\beta^2, \sigma_\epsilon^2)'$ from
 187 their full conditional distributions. SNP-based heritability estimation is performed by
 188 calculating $h_{SNP}^2 = \sigma_g^2 / (\sigma_\epsilon^2 + \sigma_g^2)$, where the genetic variance σ_g^2 is calculated as $\text{Var}(\mathbf{X}\beta)$
 189 for each sampled set of $\beta^{(i)}$ in iteration i of the MCMC chain (see Supplemental Note for
 190 further details).

191 To illustrate why the Gibbs sampling routine proposed lends itself to the use of summary
 192 statistics, we focus on the full conditional distribution of β_j under the proposed multiple
 193 regression model. To facilitate the explanation we make the simplifying assumption
 194 that $C = 2$ and $\gamma = (\gamma_1, \gamma_2) = (0, 1)$. The full conditional distribution of β_j under this
 195 assumption (see Supplemental Note) is

$$f(\beta_j | \theta_{-\beta_j}, \mathbf{y}) \propto \exp \left[-\frac{1}{2} \frac{(\beta_j - \hat{\beta}_j)^2}{\sigma_\epsilon^2 / l_j} \right], \quad (6)$$

196 where $l_j = (\mathbf{x}'_j \mathbf{x}_j + \sigma_\epsilon^2 / \sigma_\beta^2)$ and $\hat{\beta}_j = \mathbf{x}'_j \mathbf{w} / l_j$. The term l_j only involves the diagonal
 197 elements of $\mathbf{X}'\mathbf{X}$ and is easily calculated from summary statistics via $\mathbf{X}'\mathbf{X} = \mathbf{D}^{\frac{1}{2}} \mathbf{B} \mathbf{D}^{\frac{1}{2}}$. For

198 $\hat{\beta}_j$, we require $\mathbf{x}'_j \mathbf{w}$, which is defined as

$$r_j = \mathbf{x}'_j \mathbf{w} = \mathbf{x}'_j [\mathbf{y} - \mathbf{X}_{-j} \boldsymbol{\beta}_{-j}], \quad (7)$$

199 where \mathbf{X}_{-j} is \mathbf{X} without the j th column. This quantity can be efficiently stored and calculated in each MCMC iteration via a right-hand side updating scheme. We define the right-hand side $\mathbf{X}'\mathbf{y}$ corrected for all current $\boldsymbol{\beta}$ as

$$\mathbf{r}^* = \mathbf{X}'\mathbf{y} - \mathbf{X}'\mathbf{X}\boldsymbol{\beta}, \quad (8)$$

200 where \mathbf{r}^* is a vector of dimension $p \times 1$. The j th element of \mathbf{r}^* can be used to calculate

$$r_j = \mathbf{x}'_j \mathbf{w} = r_j^* + \mathbf{x}'_j \mathbf{x}_j \beta_j. \quad (9)$$

201 Therefore, once a variant has been chosen to be in the model its effect is sampled from (6),
 202 which is the kernel of the normal distribution with mean $\hat{\beta}_j$ and variance σ_e^2 / l_j (see the
 203 Supplemental Note for more detail). After the effect for variant j has been sampled we
 204 update

$$(\mathbf{r}^*)^{(i+1)} = (\mathbf{r}^*)^{(i)} - \mathbf{X}'\mathbf{x}_j(\beta_j^{(i+1)} - \beta_j^{(i)}). \quad (10)$$

205 Importantly, after the initial reconstruction of $\mathbf{X}'\mathbf{y} = \mathbf{D}\mathbf{b}$ from summary statistics, equation
 206 (10) only requires $\mathbf{X}'\mathbf{x}_j$, which is the j th column of $\mathbf{X}'\mathbf{X}$. The operation in (10) is a very
 207 efficient vector subtraction and only requires the subtraction of the non-zero elements of
 208 the shrinkage estimator of the LD correlation matrix from Wen and Stephens³⁶, which we
 209 perform using sparse matrix operations. The other elements of the Gibbs sampling routine
 210 are the same as the individual data model except for the sampling of σ_e^2 , which is outlined
 211 in the Supplemental Note.

212 **Genome-wide simulation study**

213 Before performing simulations using genome-wide variants, we first thoroughly tested
214 and compared individual level and summary statistics based methods using a simulation
215 study on two chromosomes (Supplemental Note and Figures [S1](#), [S2](#), [S3](#) and [S4](#)). This
216 small-scale simulation established the implementation of the method by comparing the
217 individual data BayesR method with SBayesR using the full LD matrix constructed from
218 the cohort used to perform the GWAS, which should theoretically give equivalent results.
219 Furthermore, it allowed for a thorough investigation of the method's properties as a
220 function of genetic architecture and LD reference in reasonable computing time relative
221 to genome-wide analyses. In particular, we observed that SBayesR outperformed other
222 summary statistics methods when the genetic architecture of the simulated trait contained
223 very large genetic effects and a polygenic background, which is expected due to the very
224 flexible SBayesR prior (Supplemental Figure [S3](#)). Overall at the scale of two chromosomes,
225 SBayesR generally outperformed other methods in terms of prediction accuracy and
226 performed well at h_{SNP}^2 estimation.

227 To investigate the performance of the methodology at a genome-wide scale, we simu-
228 lated quantitative phenotypes using 1,094,841 genome-wide HM3 variants and a random
229 subset of 100,000 individuals from the 348,580 unrelated European ancestry individuals in
230 the UKB data set. For the same set of 1,094,841 variants, we generated two independent
231 tuning and validation genotype sets from the remaining 248,580 unrelated European indi-
232 viduals each containing 10,000 individuals. The 1,094,841 variant subset was formed from
233 the 1,365,446 HM3 SNPs further filtered on $MAF > 0.01$, strand ambiguous SNPs (as do
234 Vilhjálmsson *et al.*⁴⁴ and Bulik-Sullivan *et al.*³⁹), removal of long-range LD regions (defined
235 in Bycroft *et al.*⁵⁰ Table S13 and includes the MHC), which increased model stability across
236 a large set of phenotypes, and overlapped with the 1000G genetic map downloaded from
237 [joepickrell/1000-genomes-genetic-maps](#). The 1000G genetic map is required for use in the
238 LD matrix shrinkage estimator³⁶. The genetic map files contain interpolated map positions
239 for the CEU population generated from the 1000G OMNI arrays. The shrinkage estimator

240 of the LD matrix³⁶, shrinks the off-diagonal entries of the LD correlation matrix toward
241 zero and is required for the Regression with Summary Statistics (RSS)⁴² and SBayesR
242 methods.

243 The simulation study on two chromosomes established that the LD reference cohort from
244 50,000 random individuals from the UKB gave the highest prediction accuracy and lowest
245 bias in h_{SNP}^2 estimation (Supplemental Note). The overlap between this random subsample
246 with the 100,000 random individuals used to generate the simulated phenotypes was 13,967.
247 For this LD reference cohort, chromosome-wise LD matrices i.e., all inter chromosomal
248 LD is ignored, were built and the shrinkage estimator of the LD matrix calculated using
249 an efficient implementation in the GCTB software. The calculation of the shrunk LD
250 matrix requires the effective population sample size, which we set to be 11,400 (as in
251 Zhu and Stephens⁴²), the sample size of the genetic map reference, which corresponds
252 to the 183 individuals from the CEU cohort of the 1000G and the hard threshold on the
253 shrinkage value, which we set to 10^{-3} . This threshold gave a good balance between
254 computational efficiency and accuracy with, on average, each SNP having 4,113 (SD=1,211)
255 non-zero elements across the autosomes (Figure S5). We further stored the shrunk LD
256 matrix in sparse matrix format (ignoring matrix elements equal to 0) for efficient SBayesR
257 computation. For LDpred⁴⁴, SBLUP⁴⁵ and PLINK clumping and then p -value thresholding
258 (P+T) (implemented in the PLINK 2 software⁴⁷), a separate genotype data set is required
259 for LD correlation reference and utilisation within each method's program. This was set
260 to be the same set of genotypes from 50,000 individual used to calculate the LD reference
261 matrix for SBayesR and RSS.

262 Two genetic architecture scenarios were generated: 10,000 causal variants sampled
263 under the SBayesR model i.e., 2500, 5000, and 2500 variants from each of $N(0, 0.01\sigma_\beta^2)$,
264 $N(0, 0.1\sigma_\beta^2)$, and $N(0, \sigma_\beta^2)$ distributions respectively and $\sigma_\beta^2 = 1$. For the second architecture,
265 50,000 causal variants were sampled from a single standard normal distribution. For each
266 replicate a new sample of causal variants was chosen at random from the set of 1,094,841
267 variants. For each scenario, 10 simulation replicates were generated under the multiple

268 regression model using the phenotype simulation tool in the GCTA software⁵⁸ and centred
269 and scaled genotypes for all 100,000 individuals. For each architecture the residual variance
270 was scaled such that the total h_{SNP}^2 was 0.1, 0.2 and 0.5, which led to a total of six simulation
271 scenarios.

272 For each of the six scenarios, simple linear regression for each variant was run using
273 the -linear option in the PLINK 2 software for each of the 10 simulation replicates to
274 generate summary statistics. For each of the simulation scenarios the following methods
275 were used to estimate the genetic effects: LDpred, RSS, SBLUP, P+T, BayesR³¹, and SBayesR.
276 For h_{SNP}^2 comparison we ran LD score regression (LDSC)³⁹ and Haseman-Elston regression
277 (HEreg) in the GCTA software^{48,59}. HEreg requires a GRM, which was built from the
278 1,094,841 genome-wide HM3 variants in the GCTA software. For LDpred, we specified
279 h_{SNP}^2 to be equal to the true simulated value, specified the number of SNPs on each side of
280 the focal SNP for which LD should be adjusted to be 350 (approximately 1,094,841/3,000
281 as suggested by Vilhjálmsdóttir *et al.*⁴⁴), and calculated effect size estimates for all of the
282 10 fraction of non-zero effects pre-specified parameters, which included LDpred-inf, 1,
283 0.3, 0.1, 0.03, 0.01, 0.003, 0.001, 0.0003, and 0.0001. For RSS, analyses were performed for
284 each chromosome with the chromosome-wise shrunk LD matrices calculated in GCTB and
285 stored in MATLAB format. The RSS-BSLMM model was run for 2 million MCMC iterations
286 with 1 million as burn in and a thinning rate of 1 in 100 to arrive at 10,000 posterior samples
287 for each of the model parameters. For each chromosome, the posterior mean over posterior
288 samples for the SNP effects and h_{SNP}^2 estimates was used. The chromosome wise h_{SNP}^2
289 estimates were summed to get the genome-wide estimate. For SBLUP, we used the GCTA
290 software implementation and set the shrinkage parameter $\lambda = m(1/h_{SNP}^2 - 1)$ for each true
291 simulated $h_{SNP}^2 = (0.1, 0.2, 0.5)$ and $m = 1,094,841$ and the LD window size specification
292 was set to 1 MB. LDSC was run using LD scores calculated from the 1000G Europeans
293 provided by the software and h_{SNP}^2 estimation performed. For P+T, we used the PLINK 2
294 software to clump the GWAS summary statistics discarding variants within 1 MB of and
295 in LD $R^2 > 0.1$ with the most associated SNP in the region. Using these clumped results,

296 we generated polygenic risk scores for sets of SNPs at the following p -value thresholds:
297 $5 \times 10^{-8}, 1 \times 10^{-6}, 1 \times 10^{-4}, 0.001, 0.01, 0.05, 0.1, 0.2, 0.5$, and 1.0. BayesR was run using
298 a mixture of four normal distributions model with distribution variance weights $\gamma = (0,$
299 $10^{-4}, 10^{-3}, 10^{-2})'$. BayesR was run for 4,000 iterations with 2,000 taken as burn in and a
300 thinning rate of 1 in 10. For SBayesR, the MCMC chain was run for 4,000 iterations with
301 2,000 taken as burn in and a thinning rate of 1 in 10 and run with four distributions and
302 variance weights $\gamma = (0, 0.01, 0.1, 1)'$. The posterior mean of the effects and the proportion
303 of variance explained over the 200 posterior samples was taken as the parameter estimate
304 for each scenario replicate for both methods.

305 To assess prediction accuracy, we calculated the EGV (using the score function in the
306 PLINK 2 software) for each individual using the genotypes from the 10,000 individual
307 tuning and validations data sets and the genetic effects estimated from each method.
308 Parameter tuning was performed for LDpred and P+T, where for each simulation replicate
309 the prediction accuracy was assessed for each of the pre-specified fraction of non-zero
310 effects parameters for LDpred and the p -value thresholds for P+T. The parameter that
311 gave the maximum prediction R^2 in the tuning data set was then used for calculating the
312 EGV for each individual in the validation data set. SNP effects from BayesR and SBayesR
313 were estimated using scaled genotypes and thus each variant's effect was divided by
314 $\sqrt{2q_j(1 - q_j)}$, where q_j is the minor allele frequency from the validation cohort of the j th
315 variant, before PLINK scoring was performed. The prediction R^2 was calculated via linear
316 regression of the true simulated phenotype on that predicted from each method.

317 ***Application to 10 quantitative traits in the UK Biobank***

318 To assess the methodology in real data, we performed five-fold cross-validation using
319 phenotypes and genotypes from 348,580 unrelated individuals of European ancestry from
320 the full release of the UKB data set. We chose 10 quantitative traits including: standing
321 height ($n=347,106$), basal metabolic rate (BMR, $n=341,819$), heel bone mineral density
322 T-score (hBMD, $n=197,789$), forced vital capacity (FVC, $n=317,502$), body mass index (BMI,
323 $n=346,738$), body fat percentage (BFP, $n=341,633$), forced expiratory volume in one-second

324 (FEV, $n=317,502$), hip circumference (HC, $n=347,231$), waist-to-hip ratio (WHR, $n=347,198$)
325 and birth weight (BW, $n=197,778$). All phenotypes were pre-adjusted for age, sex and the
326 first ten principal components using the R programming language⁶⁰. Principal components
327 were calculated using high-quality genotyped variants as defined in Bycroft *et al.*⁵⁰ that
328 passed additional quality control filters (as applied in the European unrelated UKB data)
329 that were LD pruned ($R^2 < 0.1$) and had long-range LD regions removed (Bycroft *et al.*⁵⁰
330 Table S13) leaving 137,102 SNPs for principal component calculation in the European
331 unrelated individuals using flashPCA⁶¹. Following covariate correction the residuals were
332 standardised to have mean zero and unit variance and finally rank-based inverse-normal
333 transformed. A set of 5,000 individuals was kept separate for LDpred and P+T parameter
334 tuning. To perform the cross-validation, the remaining 343,580 individuals were randomly
335 partitioned into five equal sized disjoint subsamples. For each fold analysis, a single
336 subsample was retained for validation with the remaining four subsamples used as the
337 training data. This process was repeated five times, with each of the five subsamples used
338 exactly once as the validation data. The SNP set used for analysis was the same set of
339 1,094,841 HM3 variants described in the genome-wide simulation study.

340 We generated summary statistics for each pre-adjusted trait in the training sample
341 in each fold by using PLINK 2 to run simple linear regression for all variants. Using
342 the individual level data and the summary statistics we performed analyses using the
343 following methods: LDpred, RSS, SBLUP, P+T, BayesR, and SBayesR. For h_{SNP}^2 comparison
344 we ran LDSC and HEreg. The same shrunk sparse reference LD correlation matrix from
345 the genome-wide simulation study was used for SBayesR and RSS analyses. For LDpred,
346 we specified the number of SNPs on each side of the focal SNP for which LD should
347 be adjusted to be 350, and calculated effect size estimates for all of the 10 fraction of
348 non-zero effects pre-specified parameters, which included LDpred-inf, 1, 0.3, 0.1, 0.03,
349 0.01, 0.003, 0.001, 0.0003, and 0.0001. The optimal parameter was chosen by predicting
350 into the independent subset of 5,000 individuals initially partitioned off and choosing that
351 which had the highest prediction R^2 when the predicted phenotype was regressed on the

352 true simulated phenotype. For RSS, analyses were performed for each chromosome with
353 the chromosome-wise shrunk LD matrices calculated in GCTB and stored in MATLAB
354 format. The RSS-BSLMM model was run for 2 million MCMC iterations with 1 million as
355 burn in and a thinning rate of 1 in 100 to arrive at 10,000 posterior samples for each of the
356 model parameters. For each chromosome, the posterior mean over posterior samples for
357 the SNP effects and h_{SNP}^2 estimates was used. The chromosome wise h_{SNP}^2 estimates were
358 then summed to get the genome-wide estimate. For SBLUP, we used the GCTA software
359 implementation, which requires the specification of the $\lambda = m(1/h_{SNP}^2 - 1)$ parameter.
360 For each fold, h_{SNP}^2 was taken to be the estimate from HEreg and $m = 1,094,841$. The LD
361 window size specification was set to 1 MB for ease of computation. SBLUP and LDpred
362 were run on each chromosome separately to improve computational efficiency. LDSC was
363 run using LD scores from the 1000G European data and h_{SNP}^2 estimation performed. For
364 P+T, we ran the same clumping procedure and calculated polygenic risk scores for the
365 same set of p -value thresholds as in the simulation studies. BayesR and SBayesR were
366 run using the same protocols as in the simulation studies. SNP effects from BayesR and
367 SBayesR were again rescaled before PLINK scoring was performed.

368 To assess prediction accuracy, we calculated EGVs using the genotype data from the
369 independent validation retained set in each fold. The PLINK 2 software was used to
370 calculate EGVs for all methods and the prediction R^2 calculated via linear regression of
371 the true phenotype on that calculated from each method.

372 **Across biobank prediction analysis**

373 To investigate how the proposed methods scale and perform in very large data sets, we
374 analysed the full set of unrelated and related ($n = 456,426$) UKB European ancestry
375 individuals and used summary statistics from the largest meta-analysis of height and
376 BMI⁴⁹. For these analyses, the same set of 1,094,841 genome-wide HM3 variants described
377 in the simulations was used. The set of traits was limited to those that were present in the
378 UKB and had large independent validation sets, which included the HRS and the ESTB⁵⁶,
379 which contain imputed genotype and phenotype information on BMI and height.

380 To generate a baseline for comparison between the individual data BayesR method
381 and the SBayesR method we first analysed data from the same set of individuals and
382 variants from the full set of unrelated and related UKB individuals. BMI and height
383 phenotypes were pre-adjusted for age, sex and the first ten principal components using
384 the R programming language as per the cross-validation. We generated summary statistics
385 for SBayesR analysis for height and BMI using a linear mixed-model to account for sample
386 relatedness in the BOLT-LMM v2.3 software ^{13,25} for the 1,094,841 HM3 variants in the full
387 UKB data set. Using these summary statistics, we ran SBayesR for 4,000 iterations with
388 2,000 taken as burn in and a thinning rate of 1 in 10 and four distributions and variance
389 weights $\gamma = (0, 0.01, 0.1, 1)'$. For comparison in the full UKB data set, we ran the individual
390 level BayesR method using a mixture of four normal distributions model with distribution
391 variance weights $\gamma = (0, 10^{-4}, 10^{-3}, 10^{-2})'$. BayesR was run for 4,000 iterations with 2,000
392 taken as burn in and a thinning rate of 1 in 10. The posterior mean of the sampled genetic
393 effects and h_{SNP}^2 over the 200 posterior samples was taken as the parameter estimate for
394 each trait for both methods.

395 Motivated by the hypothesis that summary statistics methodologies can increase pre-
396 diction accuracy over large-scale individual level analyses by utilising publicly available
397 summary statistics from very large GWASs, we took the summary statistics from the largest
398 meta-analysis of BMI and height ⁴⁹ and analysed them using SBayesR, RSS and LDpred,
399 which were the best performing summary based methods (in terms of prediction accuracy)
400 in the cross-validation. We subsetted the set of 1,094,841 HM3 variants to 982,074 vari-
401 ants that overlapped with those in both the BMI and height summary statistics sets. The
402 summary based methodology implicitly assumes that the summary statistics have been
403 generated on the same set of individuals ⁴². Empirically we observed that the methodology
404 can tolerate deviations from this assumption up to a limit. To improve method convergence
405 we removed variants from the Yengo *et al.* ⁴⁹ summary statistics that had a per variant
406 sample size that deviated substantially from the mean of the sample size distribution over
407 all variants, which was also performed by Pickrell *et al.* ⁶² and recommended by Zhu and

408 Stephens⁴². To minimise the variants removed, we interrogated the distributions of per
409 variant sample size in each of the BMI and height summary statistics sets and removed
410 variants in the lower 2.5th percentile and upper 5th percentile of the per variant sample
411 size distribution for BMI and in the lower 5th percentile for height (Figure S6). This left
412 932,969 and 909,293 variants with summary information for height and BMI respectively.
413 These sets of variants were also used in the LDpred and RSS analyses.

414 SBayesR was run as above with the default γ for BMI and $\gamma = (0, 10^{-4}, 10^{-3}, 1)'$ for
415 height. Empirically, we observed that this constraint on the elements of γ was a further
416 requirement for SBayesR model convergence using these height summary statistics. For
417 LDpred, we specified the number of SNPs on each side of the focal SNP for which LD
418 should be adjusted to be 350, and calculated effects size estimates for all of the 10 fraction
419 of non-zero effects pre-specified parameters, which included LDpred-inf, 1, 0.3, 0.1, 0.03,
420 0.01, 0.003, 0.001, 0.0003, and 0.0001. The optimal parameter was chosen by predicting
421 into the HRS data set and choosing the parameter that had the highest prediction R^2 when
422 the predicted phenotype was regressed on the true phenotype. This optimal parameter
423 was then used for prediction into the ESTB. For RSS, analyses were performed for each
424 chromosome with the chromosome-wise shrunk LD matrices from the simulation and
425 cross-validation analyses used. The RSS-BSLMM model was run for 2 million MCMC
426 iterations with 1 million as burn in and a thinning rate of 1 in 100 to arrive at 10,000
427 posterior samples for each of the model parameters. For each chromosome, the posterior
428 mean over posterior samples for the SNP effects and h_{SNP}^2 estimates was used. The
429 chromosome-wise h_{SNP}^2 estimates were then summed to get the genome-wide estimate.
430 To assess prediction accuracy, we calculated EGVs using the genotype data from the
431 independent test data sets using the PLINK 2 software for all methods. Prediction R^2 was
432 calculated via linear regression of the true phenotype on that estimated from each method,
433 which was used as a measure of prediction accuracy for each trait.

434 **Results**

435 ***Genome-wide simulation study***

436 Across the simulation scenarios, we observed that BayesR or SBayesR gave the highest or
437 equal highest mean validation prediction R^2 across the 10 replicates (Figure 1). SBayesR
438 showed the highest or equal highest mean prediction R^2 of the summary statistics method-
439 ologies across all scenarios. The difference between the mean prediction R^2 from BayesR
440 and that from SBayesR was minimal for less heritable traits with SBayesR showing a
441 marginally higher mean R^2 for lower heritable traits with 50k causal variants. Prediction
442 R^2 for BayesR was maximally greater than SBayesR when $h_{SNP}^2 = 0.5$ and for the 10k causal
443 variant scenario with a relative increase of 13.2% (from 0.356 to 0.403). P+T performed
444 well across scenarios and showed increased mean prediction R^2 relative to LDpred-inf and
445 SBLUP in the 10k causal variant scenarios but did not perform substantially better than
446 LDpred tuned for the polygenicity parameter across all scenarios. RSS showed the closest
447 mean prediction R^2 to SBayesR in the 10k causal variant simulation scenarios. Similarly,
448 SBLUP showed a mean prediction R^2 close to SBayesR in the 50k causal variant simulation
449 scenarios. SBayesR showed the largest nominally significant (p -value=0.015) improvement
450 in prediction R^2 over other summary statistics methodologies in the 10k causal variant
451 scenario and $h_{SNP}^2 = 0.5$ with an relative difference in mean of 3.5% (from 0.344 to 0.356)
452 over RSS.

453 Across all simulation scenarios, all methods except RSS showed minimal bias in h_{SNP}^2
454 estimation (Figure S7), with HEreg showing the least bias across all scenarios. SBayesR
455 maintained a small upward bias across all simulation scenarios and a maximum upward
456 relative on mean bias of 5.0% (0.105 compared to 0.1) in the 10k causal variant scenarios
457 (Figure S7). Similar to RSS, LDSC maintained a small downward bias in mean h_{SNP}^2 with a
458 maximum of relative deviation of 6.4% (0.468 compared to 0.5) for the $h_{SNP}^2 = 0.5$ and 10k
459 causal variant scenario.

460 We compared the CPU time and memory usage between all methods in each scenario.
461 P+T, HEreg and LDSC were not compared as they required minimal relative computational

462 resources but do not estimate the genetic effects. For the Bayesian methodologies, runtime
463 is dependent on the length of the MCMC chain. The chain length of 4,000 MCMC iterations
464 for BayesR was chosen as a compromise between maximum prediction accuracy and
465 computational efficiency. We observed that a marginal relative gain in the mean prediction
466 accuracy of 0.5% (e.g., 0.403 to 0.405) could be achieved if the chain was run for 10,000
467 iterations (mean runtime of 110 hours) (Figure S8) at a cost of twice the runtime. An
468 MCMC chain length of 4,000 iterations was chosen for SBayesR to allow direct comparison
469 with the results from BayesR with no improvement in mean prediction R^2 if a chain length
470 of 100,000 (mean runtime of 15 hours) was used (Figure S9). We observed substantial
471 differences between prediction accuracy results from RSS when the chain length was
472 reduced to 200,000 iterations (in an attempt to reduce computational time) (Figure S10)
473 and we thus maintained an MCMC chain length of 2 million iterations, which was used
474 in Zhu and Stephens⁴². Across the simulation scenarios, SBayesR had the shortest mean
475 runtime (approximately one hour) with a greater than 10-fold improvement over the
476 second quickest LDpred (Figure S12). SBayesR required \approx 50 GB of memory usage, which
477 was similar to SBLUP (35-40 GB), although SBLUP had a much longer on mean runtime.
478 SBayesR required half the memory of the individual data BayesR, which has been highly
479 optimised for time and memory efficiency, and showed a seven-fold improvement over
480 LDpred and a 30-fold improvement over RSS (Figure S13). We note that the memory
481 requirements for SBayesR are fixed for this set of variants for an arbitrary number of
482 individuals, which is not the case for the individual level BayesR method. The total
483 time and memory used to compute the SBayesR LD reference is not included in these
484 assessments. The building of the sparse LD reference for SBayesR took in total 13 and
485 1/3 CPU days and approximately 500 GB of memory. SBayesR can compute the sparse
486 LD matrix in parallel via dividing each chromosome into genomic ‘chunks’. We used 100
487 CPUs to compute the LD matrix, which brought the average runtime and memory for
488 computing each LD matrix chunk to 3.25 hours and 5 gigabytes. These chromosome-wise
489 LD matrices are a once off computation cost that can be distributed with the program and

490 were used for all SBayesR and RSS analysis in the genome-wide simulation and further
491 analyses using this HM3 variant set.

492 ***Application to 10 quantitative traits in the UK Biobank***

493 We compared all methods in terms of prediction accuracy and h_{SNP}^2 estimation across
494 10 quantitative traits in the UKB using five-fold cross-validation. SBayesR consistently
495 improved or equalled the mean prediction R^2 of all other methods, including the individual
496 level BayesR method, across the five folds for 8/10 traits (Figure 2). BayesR was the only
497 method to exceed SBayesR in mean prediction R^2 and showed a relative increase of 4.3%
498 (from 0.187 to 0.195) for heel BMD and 4.3% (from 0.349 to 0.364) for height. Heel BMD,
499 height and FVC showed nominal significance (p -value = (0.007, 0.029, 0.011) respectively)
500 in prediction accuracy improvement over RSS with a relative improvement in mean
501 prediction R^2 of 2.5% (from 0.182 to 0.187), 2.0% (from 0.342 to 0.349) and 2.5% (from 0.123
502 to 0.127) respectively (Figure 2). SBayesR showed larger improvements relative to LDpred
503 tuned for the polygenicity parameter with SBayesR showing mean relative prediction R^2
504 increases over LDpred ranging from 2% (BFP) to 37% (hBMD).

505 For all traits except height, h_{SNP}^2 estimates were consistent across all methods (Figure
506 S14). Across all traits except BW and FEV, SBayesR gave the highest mean h_{SNP}^2 estimate
507 and LDSC the lowest mean value, with the largest deviation in mean LDSC estimates from
508 other methods for hBMD and height. On mean across the five folds, relative deviations
509 in mean h_{SNP}^2 estimates between SBayesR and HEreg were between 1.0%-14.6% with the
510 largest deviations being for WHR (6.4%), BFP (9.7%) and BW (14.7%). Similar ranges in
511 relative deviations from mean HEreg h_{SNP}^2 estimates were observed for other methods,
512 with BayesR showing a range of 1.8%-20.1% and RSS 1.2%-23.1%.

513 We summarised the time and memory requirements of BayesR, SBayesR, RSS, LDpred
514 and SBLUP for all traits across the five folds. P+T, HEreg and LDSC are very time
515 and memory efficient and we therefore did not summarise their resource requirements.
516 SBayesR on mean took approximately one to two hours and required 50 GB of memory to
517 complete a genome wide analysis (1,094,841 HM3 variants) with variability depending

518 on the number of non-zero variants in the model (Figures 3 and S17). For example, BFP
519 and BMI had approximately 120,000 non zero effects whereas hBMD had approximately
520 30,000 and consequently the shortest runtime (Figure 3). The difference in the number
521 of non-zero effects in the model for these traits may be driven in part by the sample size
522 differences between BMI ($n=346,738$) and hBMD ($n=197,789$). RSS had the longest runtime
523 with a total on mean CPU runtime being in the order of 400 hours. Again, shortening of
524 the chain to 200,000 iterations to reduce runtime decreased the prediction accuracy of RSS
525 with marginal changes in mean h_{SNP}^2 estimates (Figures S15 and S16). LDpred was the
526 closest to SBayesR in terms of runtime with total time being 25 hours on mean across the
527 traits. SBayesR showed a six-fold memory improvement over BayesR and LDpred and a 30
528 fold improvement over RSS (Figure S17). The improvements in memory between SBayesR,
529 LDpred and SBLUP are likely a result of not having to compute the LD correlations for
530 each fold in each trait. The memory improvement over RSS is due to the sparse matrix
531 storage and computation in SBayesR.

532 ***Across biobank prediction analysis***

533 Overall, SBayesR gave similar but consistently higher prediction R^2 values than BayesR
534 for both BMI and height in both the HRS and ESTB samples (Figure 4), when the summary
535 statistics from the full European ancestry (related and unrelated individuals) UKB data
536 set were used ($n = 453,458$ and $n = 454,047$ for BMI and height respectively). When the
537 summary statistics from Yengo *et al.*⁴⁹ were used, a further improvement in prediction
538 R^2 was observed for SBayesR and RSS, except for height and in HRS (Figure 4). SBayesR
539 and RSS gave the same prediction R^2 values for BMI with marginal increases of SBayesR
540 over RSS for height, which is consistent with the results from the cross-validation. The
541 maximum increase in SBayesR prediction R^2 relative to the BayesR analysis using just
542 the UKB data for BMI was 11.3% (from 0.106 to 0.118) and 4.9% (from 0.307 to 0.322) for
543 height in the ESTB sample when the summary statistics from the⁴⁹ data set were used.
544 The maximum increase in prediction R^2 relative to that from the predictor built from the
545 GCTA-COJO analysis thresholded at p -value < 0.001 performed in Yengo *et al.*⁴⁹ for BMI

546 was 32.5% (from 0.089 to 0.118) in the ESTB. For height, we observed a maximum relative
547 increase of 31.6% (from 0.244 to 0.321) in prediction R^2 over the P+T predictor of Yengo *et*
548 *al.*⁴⁹ in the HRS sample when the summary statistics from the full UKB data set were used
549 for SBayesR analysis.

550 Discussion

551 Clinically relevant genetic predictors for complex traits and disorders will require the
552 analysis of data from large consortia and biobank initiatives, with sample sizes for GWASs
553 set to soon regularly reach into the millions of individuals. Efficient methods that produce
554 theoretically optimal predictors under the multiple regression model will therefore be
555 critical to this goal. We have presented one solution, that rests on an extension of the
556 established summary statistics methodological framework to include a class of point-
557 normal mixture prior Bayesian regression models, which encompasses many previously
558 proposed models^{27,28,31}.

559 We observed that the cohort used to construct the LD reference matrix influenced the
560 prediction accuracy and h_{SNP}^2 estimation. The LD reference built from a random sample of
561 50k individuals from the UKB showed the maximum prediction accuracy and smallest
562 upward bias in h_{SNP}^2 estimation across all scenarios in the small-scale simulation on two
563 chromosomes although these were marginal relative to those from the smaller UK10K
564 sequence reference. We anticipate that the UKB will contribute to future large-scale GWASs
565 and thus we anticipate that the LD reference built from a large subset of this cohort in this
566 study will be highly beneficial to future summary statistics analyses of complex traits.

567 The simulation studies thoroughly compared prediction methods as a function of genetic
568 architecture, LD reference and other parameters, with SBayesR generally outperforming
569 other methods. In simulation, P+T performed well across scenarios and showed increased
570 mean prediction R^2 relative to SBLUP and LDpred-inf in a subset of the simulation
571 scenarios but did not perform better than LDpred tuned for the polygenicity parameter
572 across all scenarios, which is contrary to observations made by Mak *et al.*⁴⁶. In the five-fold

573 cross-validation, SBayesR consistently improved or equalled the mean prediction R^2 of all
574 other methods, with a marginal improvement over the individual level BayesR method for
575 most traits. SBayesR maintained a minimal upward bias across all simulation scenarios
576 (maximum upward bias of $\approx 5.0\%$) and showed h_{SNP}^2 estimates close to that from HEreg
577 in the cross-validation analysis. SBayesR gave consistently higher but similar prediction
578 R^2 values than BayesR for both BMI and height in across biobank predictions into the
579 HRS and ESTB samples. This was both the case when the summary statistics from the full
580 European UKB data set were used with a further improvement in prediction R^2 observed
581 when the summary statistics from Yengo *et al.*⁴⁹ were used. The maximum increase in
582 prediction R^2 relative to the prediction R^2 from Yengo *et al.*⁴⁹ for height was in the the
583 HRS sample when the summary statistics from the full UKB data set were used 31.6%
584 (from 0.244 to 0.321). The maximal prediction accuracy in HRS and ESTB was $R^2 = 0.321$
585 (correlation between outcome and predictor of $\sqrt{0.32} = 0.57$), which is starting to reach
586 the initial estimates of h_{SNP}^2 of 0.45 in Yang *et al.*²¹.

587 The observation that SBayesR improves on the BayesR prediction accuracy in real data
588 cross-validation and independent out-of-sample prediction is contrary to expectation.
589 In the small-scale simulation we observed that SBayesR using the full LD correlation
590 matrix and BayesR, which are theoretically equivalent, returned equal on mean prediction
591 accuracies and h_{SNP}^2 estimates and thus the numerical implementation is not substantially
592 superior. When we scaled the simulation to the whole genome, we observed that BayesR
593 showed relatively smaller improvements over SBayesR for lower heritable traits in the
594 10k causal variant scenarios and for 50k causal variants scenarios SBayesR improved on
595 BayesR mean prediction R^2 for lower heritability traits, which was also the case for lower
596 heritable traits in the cross-validation. For lower heritable traits the length of the BayesR
597 MCMC chain may play a larger role with marginal improvements in prediction accuracy
598 observed for longer BayesR chains for the 10k causal variants and $h_{SNP}^2 = 0.5$ genome-
599 wide simulation scenario. A further factor is the impact of using summary statistics results
600 from a LMM (e.g., Loh *et al.*²⁵), where the model is derived under the assumption that

601 the summary statistics have been generated from a least squares analysis. The use of
602 summary statistics from a LMM will affect the reconstruction of $X'y$. One further, and
603 likely major, difference between these two methods is the ignorance of interchromosomal
604 LD in the SBayesR method, where interchromosomal LD may result from genetic sampling
605 in finite population sizes, population structure and non-random mating (e.g., assortative
606 mating). The incorporation of this information appears only advantageous for predictions
607 performed within an independent subset from the same population e.g., the partitioning
608 of the UKB in the simulation studies and in cross-validation. The HRS and ESTB data
609 are unlikely to contain the same interchromosomal LD correlation structure and thus its
610 inclusion in the BayesR analysis may be partially detrimental as it comes into the model
611 as informative within data set (UKB) but as noise across data sets (UKB to HRS/ESTB).
612 One hypothesis for this is that the HRS and ESTB populations have different patterns of
613 assortative mating for specific traits than in the UKB, or individuals in HRS or ESTB are
614 more randomly mated than in those in the UKB.

615 The method is implemented in a very efficient and user-friendly software tool that
616 maximises computational efficiency via precomputing and efficiently storing sparse LD
617 matrices that account for the variation in the number of LD ‘friends’ for each variant. In
618 simulation and cross-validation we showed large fold improvements in time and memory
619 over current state-of-the-art individual and summary data methods. The improvements in
620 efficiency are not just a result of the computational implementation but are a contributed
621 to by the faster convergence of the the Gibbs sampling algorithm. This is evidenced by the
622 comparison with RSS, which requires a much longer chain length to arrive at maximum
623 prediction accuracy. Importantly, once the GWAS effect size estimates have been generated
624 the method’s runtime is independent of the sample size making it applicable to an arbitrary
625 number of individuals.

626 We found that model convergence is sensitive to inconsistencies in summary statistics
627 generated from external consortia and meta-analyses. We observed that the shrinkage
628 estimator of the LD matrix³⁶ can assist with more stable model convergence. We observed

629 a persistent small upward bias in h_{SNP}^2 estimation, which was also observed by Zhu and
630 Stephens⁴². We did not observe this upward bias in the RSS analyses, which may in part
631 be attributed to the much larger LD reference used. Zhu and Stephens⁴² hypothesised
632 that the persistent upward inflation to be due to deviations from the assumption of small
633 effects underlying the RSS model. However, we did not observe large differences in
634 upward bias in h_{SNP}^2 estimation between simulation scenarios containing very large effects
635 compared to scenarios with effect sizes similar to those for very polygenic traits. It is
636 difficult to assess the impact of the small effect assumption versus the contribution from the
637 replacement of the **D** and LD matrices with estimates reconstructed from GWAS summary
638 statistics from external references or a subset of the GWAS data. Through simulation,
639 we observed that this upward bias can be minimised through an optimally sparse and
640 sufficiently large LD reference. The impact from residual population stratification in the
641 GWAS summary statistics is another potential source in upward bias in h_{SNP}^2 estimates
642 but was not investigated via simulation.

643 There are distinct practical advantages in estimating h_{SNP}^2 and the genetic effects within
644 one framework with the method encompassing many available summary statistics method-
645 ologies. Zhu and Stephens⁴² presented a similar omnibus method and showed the ca-
646 pacity of this similar methodology for variant mapping. Although we haven't assessed
647 our method's effectiveness for mapping causal variants we expect it to be capable of
648 performing this task, which is to be inherited from the individual-level BayesR method's
649 capacity to perform this task^{31,63,64}. SBayesR estimates all parameters from the data and
650 does not require any post-hoc tuning of prediction relevant parameters in a test data subset
651 (as in the polygenicity parameter in LDpred or P+T), which has practical advantages in
652 terms of relieving the analytical burden of tuning these parameters in an external data
653 set. Furthermore, this leads to more generalisable predictors as the parameters have been
654 optimised over all possible values rather than selected from a finite grid.

655 The method assumes certain ideal data constraints such as summary data computed from
656 a single set of individuals at fully observed genotypes as well as minimal imputation error

and data processing errors such as allele coding and frequency mismatch. Summary data in the public domain often substantially deviate from these ideals and can contain residual population stratification, which is not accounted for in this model. Practical solutions to these ideal data deviations include the use of data that are imputed and the restriction of analyses to variants that are known to be imputed with high accuracy as in Bulik-Sullivan *et al.*³⁹ and Zhu and Stephens⁴². We found that the simple filtering of SNPs with sample sizes that deviate substantially from the mean across all variants from an analysis, as in Pickrell *et al.*⁶², when using summary statistics from the public domain substantially improved model convergence. We explored LD pruning of variants to remove variants in very high LD ($R^2 > 0.99$) but found that this did not substantially improve model convergence or parameter estimates although this was not formally assessed. However, removal of high LD regions, such as the MHC region improved model convergence for real traits. High LD regions are expected to have the potential to be extreme sources of model misspecification with the model expecting summary data in to be very similar for variants in high LD. Small deviations due to data error not expected in the model likelihood at these loci thus have high potential to lead to model divergence (see Zhu and Stephens⁴² for further discussion). Future research into efficient diagnostic tools and methods that can assist analysts with the assessment of sources of bias and error and summary data quality would be highly beneficial.

We expect that as GWAS sample sizes continue to grow that polygenic predictions will become more accurate. We expect that they will be important in future clinical settings, for improving prediction in diverse populations and for understanding quantitative genetics more generally. The very efficient implementation of our method makes the analysis of millions of variants and an arbitrary number of individuals possible. The implementation and model are very flexible and can easily incorporate other model formalisations such as understanding the contributions of genomic annotations to prediction and h_{SNP}^2 enrichment such as in^{41,65} or understanding genetic architecture via summary statistics versions of models such as those presented in Gazel *et al.*⁶⁶ and Zeng *et al.*³⁰.

685 Acknowledgements

686 The authors would like to thank the members of the Program in Complex Genetics
687 for their insights and helpful discussion. We are grateful to Xiang Zhu for assistance
688 and discussion concerning the Residual with Summary Statistics methodology. The
689 authors would like to acknowledge the support from the Australian Research Coun-
690 cil (DP160102400), the Australian National Health and Medical Research Council (1113400,
691 1078037, 1078901 and 1080157), the National Institute of Health (R21 ES025052 and R01
692 MH100141) and the Sylvia & Charles Viertel Charitable Foundation. We gratefully acknowl-
693 edge CQU's eResearch support and the use of the High Performance Computing facility
694 (www.cqu.edu.au/hpc) in developing the updated BayesR software. **UKB:** This study
695 has been conducted using UK Biobank resource under Application Number 12514. UK
696 Biobank was established by the Wellcome Trust medical charity, Medical Research Council,
697 Department of Health, Scottish Government and the Northwest Regional Development
698 Agency. It has also had funding from the Welsh Assembly Government, British Heart
699 Foundation and Diabetes UK. **ARIC:** The Atherosclerosis Risk in Communities Study
700 is carried out as a collaborative study supported by National Heart, Lung, and Blood
701 Institute contracts (HHSN268201100005C, HHSN268201100006C, HHSN268201100007C,
702 HHSN268201100008C, HHSN268201100009C, HHSN268201100010C, HHSN268201100011C,
703 and HHSN268201100012C), R01HL087641, R01HL59367 and R01HL086694; National
704 Human Genome Research Institute contract U01HG004402; and National Institutes of
705 Health contract HHSN268200625226C. The authors thank the staff and participants of the
706 ARIC study for their important contributions. Infrastructure was partly supported by
707 Grant Number UL1RR025005, a component of the National Institutes of Health and NIH
708 Roadmap for Medical Research. **UK10K:** The UK10K project was funded by the Wellcome
709 Trust award WT091310. Twins UK (TUK): TUK was funded by the Wellcome Trust and
710 ENGAGE project grant agreement HEALTH-F4-2007-201413. The study also receives
711 support from the Department of Health via the National Institute for Health Research
712 (NIHR)-funded BioResource, Clinical Research Facility and Biomedical Research Centre

713 based at Guy's and St. Thomas' NHS Foundation Trust in partnership with King's College
714 London. Dr Spector is an NIHR senior Investigator and ERC Senior Researcher. Funding
715 for the project was also provided by the British Heart Foundation grant PG/12/38/29615
716 (Dr Jamshidi). A full list of the investigators who contributed to the UK10K sequencing
717 is available from www.UK10K.org. **HRS:** HRS is supported by the National Institute
718 on Aging (NIA U01AG009740). The genotyping was funded separately by the National
719 Institute on Aging (RC2 AG036495, RC4 AG039029). Genotyping was conducted by the
720 NIH Center for Inherited Disease Research (CIDR) at Johns Hopkins University. Geno-
721 typing quality control and final preparation of the data were performed by the Genetics
722 Coordinating Center at the University of Washington. **ESTB:** The Estonian Genome Centre
723 of University of Tartu Study was supported by EU Horizon 2020 grants 692145, 676550,
724 and 654248; Estonian Research Council Grant IUT20-60, NIASC, EIT Health; NIH BMI
725 grant 2R01DK075787-06A1; and the European Regional Development Fund (project 2014-
726 2020.4.01.15-0012 GENTRANSMED).

727 **Author contributions**

728 P.M.V., J.Y., M.E.G. and N.R.W. conceived the study. P.M.V., J.Y., L.R.L-J and J.Z. designed
729 the experiment. J.Z., L.R.L-J and M.E.G. derived the analytical methods. L.R.L-J and J.Z.
730 conducted all analyses with assistance from J.S. and guidance from P.M.V., J.Y., L.Y., G.M.,
731 and H.W. J.Z. and L.R.L-J developed the GCTB software. G.M. developed the updated
732 version of the BayesR software. K.E.K, L.Y. and Z.Z. performed the initial preparation and
733 quality control of the UK Biobank data. J.S., R.M., T.E., and A.M supplied and performed
734 initial quality control on the Estonian Biobank data. L.R.L-J wrote the manuscript with
735 the participation of all authors in particular P.M.V., J.Y., and J.Z. All authors reviewed and
736 approved the final manuscript.

737 References

738 [1] Wray, N. R., Goddard, M. E. & Visscher, P. M. Prediction of individual genetic risk of
739 complex disease. *Current Opinion in Genetics & Development* **18**, 257–263 (2008).

740 [2] Katsanis, S. H. & Katsanis, N. Molecular genetic testing and the future of clinical
741 genomics. *Nature Reviews Genetics* **14**, 415 (2013).

742 [3] Aronson, S. J. & Rehm, H. L. Building the foundation for genomics in precision
743 medicine. *Nature* **526**, 336 (2015).

744 [4] Chatterjee, N., Shi, J. & García-Closas, M. Developing and evaluating polygenic risk
745 prediction models for stratified disease prevention. *Nature Reviews Genetics* **17**, 392
746 (2016).

747 [5] Torkamani, A., Wineinger, N. E. & Topol, E. J. The personal and clinical utility of
748 polygenic risk scores. *Nature Reviews Genetics* **1** (2018).

749 [6] Wray, N. R., Goddard, M. E. & Visscher, P. M. Prediction of individual genetic risk to
750 disease from genome-wide association studies. *Genome Research* **17** (2007).

751 [7] Abraham, G. & Inouye, M. Genomic risk prediction of complex human disease and
752 its clinical application. *Current Opinion in Genetics & Development* **33**, 10–16 (2015).

753 [8] Visscher, P. M. *et al.* 10 years of GWAS discovery: biology, function, and translation.
754 *The American Journal of Human Genetics* **101**, 5–22 (2017).

755 [9] Pasaniuc, B. & Price, A. L. Dissecting the genetics of complex traits using summary
756 association statistics. *Nature Reviews Genetics* **18**, 117 (2017).

757 [10] Wray, N. R. *et al.* Pitfalls of predicting complex traits from SNPs. *Nature Reviews
758 Genetics* **14**, 507 (2013).

759 [11] Sudlow, C. *et al.* UK Biobank: an open access resource for identifying the causes of a
760 wide range of complex diseases of middle and old age. *PLoS Medicine* **12**, e1001779
761 (2015).

762 [12] Lee, J. J. *et al.* Gene discovery and polygenic prediction from a genome-wide associa-
763 tion study of educational attainment in 1.1 million individuals. *Nature Genetics* **50**,
764 1112–1121 (2018).

765 [13] Loh, P.-R., Kichaev, G., Gazal, S., Schoech, A. P. & Price, A. L. Mixed-model association
766 for biobank-scale datasets. *Nature Genetics* **50**, 906–908 (2018).

767 [14] Purcell, I., Sean M *et al.* Common polygenic variation contributes to risk of schizophrenia
768 and bipolar disorder. *Nature* **460**, 748 (2009).

769 [15] Dudbridge, F. Power and predictive accuracy of polygenic risk scores. *PLoS Genetics*
770 **9**, e1003348 (2013).

771 [16] Wray, N. R. *et al.* Research review: polygenic methods and their application to
772 psychiatric traits. *Journal of Child Psychology and Psychiatry* **55**, 1068–1087 (2014).

773 [17] Euesden, J., Lewis, C. M. & O'reilly, P. F. PRSice: polygenic risk score software.
774 *Bioinformatics* **31**, 1466–1468 (2014).

775 [18] Robinson, G. K. That BLUP is a good thing: The estimation of random effects.
776 *Statistical Science* 15–32 (1991).

777 [19] Goddard, M. E., Wray, N. R., Verbyla, K., Visscher, P. M. *et al.* Estimating effects and
778 making predictions from genome-wide marker data. *Statistical Science* **24**, 517–529
779 (2009).

780 [20] De Los Campos, G., Gianola, D. & Allison, D. B. Predicting genetic predisposition
781 in humans: the promise of whole-genome markers. *Nature Reviews Genetics* **11**, 880
782 (2010).

783 [21] Yang, J. *et al.* Common SNPs explain a large proportion of the heritability for human
784 height. *Nature Genetics* **42**, 565–569 (2010).

785 [22] Speed, D., Hemani, G., Johnson, M. R. & Balding, D. J. Improved heritability estimation
786 from genome-wide SNPs. *The American Journal of Human Genetics* **91**, 1011–1021
787 (2012).

788 [23] Vilhjálmsson, B. J. & Nordborg, M. The nature of confounding in genome-wide
789 association studies. *Nature Reviews Genetics* **14**, 1–2 (2013).

790 [24] Yang, J., Zaitlen, N. A., Goddard, M. E., Visscher, P. M. & Price, A. L. Advantages and
791 pitfalls in the application of mixed-model association methods. *Nature Genetics* **46**,
792 100–106 (2014).

793 [25] Loh, P.-R. *et al.* Efficient Bayesian mixed-model analysis increases association power
794 in large cohorts. *Nature Genetics* **47**, 284–290 (2015).

795 [26] Meuwissen, T. H. E., Hayes, B. J. & Goddard, M. E. Prediction of total genetic value
796 using genome-wide dense marker maps. *Genetics* **157**, 1819–1829 (2001).

797 [27] Habier, D., Fernando, R. L., Kizilkaya, K. & Garrick, D. J. Extension of the Bayesian
798 alphabet for genomic selection. *BMC Bioinformatics* **12**, 1 (2011).

799 [28] Erbe, M. *et al.* Improving accuracy of genomic predictions within and between dairy
800 cattle breeds with imputed high-density single nucleotide polymorphism panels.
801 *Journal of Dairy Science* **95**, 4114–4129 (2012).

802 [29] Zhou, X., Carbonetto, P. & Stephens, M. Polygenic modeling with Bayesian sparse
803 linear mixed models. *PLoS Genetics* **9**, e1003264 (2013).

804 [30] Zeng, J. *et al.* Signatures of negative selection in the genetic architecture of human
805 complex traits. *Nature Genetics* **50**, 746 (2018).

806 [31] Moser, G. *et al.* Simultaneous discovery, estimation and prediction analysis of complex
807 traits using a Bayesian mixture model. *PLoS Genetics* **11**, e1004969 (2015).

808 [32] Park, J.-H. *et al.* Estimation of effect size distribution from genome-wide association
809 studies and implications for future discoveries. *Nature Genetics* **42**, 570 (2010).

810 [33] Zhang, Y., Qi, G., Park, J.-H. & Chatterjee, N. Estimation of complex effect-size
811 distributions using summary-level statistics from genome-wide association studies
812 across 32 complex traits. *Nature Genetics* **50**, 1318 (2018).

813 [34] Yang, J. *et al.* Conditional and joint multiple-SNP analysis of GWAS summary statistics
814 identifies additional variants influencing complex traits. *Nature Genetics* **44**, 369–375
815 (2012).

816 [35] Benner, C. *et al.* Prospects of fine-mapping trait-associated genomic regions by using
817 summary statistics from genome-wide association studies. *The American Journal of
818 Human Genetics* **101**, 539–551 (2017).

819 [36] Wen, X. & Stephens, M. Using linear predictors to impute allele frequencies from
820 summary or pooled genotype data. *The Annals of Applied Statistics* **4**, 1158 (2010).

821 [37] Lee, D., Bigdeli, T. B., Riley, B. P., Fanous, A. H. & Bacanu, S.-A. DIST: direct im-
822 putation of summary statistics for unmeasured SNPs. *Bioinformatics* **29**, 2925–2927
823 (2013).

824 [38] Pasaniuc, B. *et al.* Fast and accurate imputation of summary statistics enhances
825 evidence of functional enrichment. *Bioinformatics* **30**, 2906–2914 (2014).

826 [39] Bulik-Sullivan, B. K. *et al.* LD score regression distinguishes confounding from
827 polygenicity in genome-wide association studies. *Nature Genetics* **47**, 291 (2015).

828 [40] Bulik-Sullivan, B. *et al.* An atlas of genetic correlations across human diseases and
829 traits. *Nature Genetics* **47**, 1236 (2015).

830 [41] Finucane, H. K. *et al.* Partitioning heritability by functional annotation using genome-
831 wide association summary statistics. *Nature Genetics* **47**, 1228 (2015).

832 [42] Zhu, X. & Stephens, M. Bayesian large-scale multiple regression with summary
833 statistics from genome-wide association studies. *The Annals of Applied Statistics* **11**,
834 1561 (2017).

835 [43] Speed, D. & Balding, D. J. SumHer better estimates the SNP heritability of complex
836 traits from summary statistics. *Nature Genetics* **1** (2018).

837 [44] Vilhjálmsdóttir, B. J. *et al.* Modeling linkage disequilibrium increases accuracy of
838 polygenic risk scores. *The American Journal of Human Genetics* **97**, 576–592 (2015).

839 [45] Robinson, M. R. *et al.* Genetic evidence of assortative mating in humans. *Nature
840 Human Behaviour* **1**, 0016 (2017).

841 [46] Mak, T. S. H., Porsch, R. M., Choi, S. W., Zhou, X. & Sham, P. C. Polygenic scores via
842 penalized regression on summary statistics. *Genetic Epidemiology* **41**, 469–480 (2017).

843 [47] Chang, C. C. *et al.* Second-generation PLINK: rising to the challenge of larger and
844 richer datasets. *Gigascience* **4**, 7 (2015).

845 [48] Haseman, J. & Elston, R. The investigation of linkage between a quantitative trait and
846 a marker locus. *Behavior Genetics* **2**, 3–19 (1972).

847 [49] Yengo, L. *et al.* Meta-analysis of genome-wide association studies for height and body
848 mass index in ~700000 individuals of European ancestry. *Human Molecular Genetics*

849 27, 3641–3649 (2018). URL <http://dx.doi.org/10.1093/hmg/ddy271>. /oup/backfile/content_

850 public/journal/hmg/27/20/10.1093_hmg_ddy271/2/ddy271.pdf.

851 [50] Bycroft, C. *et al.* The UK Biobank resource with deep phenotyping and genomic data.

852 *Nature* **562**, 203 (2018).

853 [51] ARIC Investigators. The atherosclerosis risk in community (aric) Study: Design and

854 objectives. *American Journal of Epidemiology* **129**, 687–702 (1989).

855 [52] 1000 Genomes Project Consortium *et al.* A global reference for human genetic variation.

856 *Nature* **526**, 68 (2015).

857 [53] UK10K consortium. The UK10K project identifies rare variants in health and disease.

858 *Nature* **526**, 82 (2015).

859 [54] Yang, J. *et al.* Genetic variance estimation with imputed variants finds negligible

860 missing heritability for human height and body mass index. *Nature Genetics* **47**, 1114

861 (2015).

862 [55] Sonnega, A. *et al.* Cohort profile: The health and retirement study (HRS). *International*

863 *Journal of Epidemiology* **43**, 576–585 (2014).

864 [56] Leitsalu, L. *et al.* Cohort profile: Estonian biobank of the Estonian Genome center,

865 University of Tartu. *International Journal of Epidemiology* **44**, 1137–1147 (2014).

866 [57] Mitt, M. *et al.* Improved imputation accuracy of rare and low-frequency variants using

867 population-specific high-coverage wgs-based imputation reference panel. *European*

868 *Journal of Human Genetics* **25**, 869 (2017).

869 [58] Yang, J., Lee, S. H., Goddard, M. E. & Visscher, P. M. GCTA: a tool for genome-wide

870 complex trait analysis. *The American Journal of Human Genetics* **88**, 76–82 (2011).

871 [59] Yang, J., Zeng, J., Goddard, M. E., Wray, N. R. & Visscher, P. M. Concepts, estimation

872 and interpretation of SNP-based heritability. *Nature Genetics* **49**, 1304 (2017).

873 [60] R Core Team. *R: A Language and Environment for Statistical Computing*. R Foundation

874 for Statistical Computing, Vienna, Austria (2016). URL <https://www.R-project.org/>.

875 [61] Abraham, G. & Inouye, M. Fast principal component analysis of large-scale genome-

876 wide data. *PloS One* **9**, e93766 (2014).

877 [62] Pickrell, J. K. Joint analysis of functional genomic data and genome-wide association
878 studies of 18 human traits. *The American Journal of Human Genetics* **94**, 559–573 (2014).

879 [63] Lloyd-Jones, L. R. *et al.* Inference on the genetic basis of eye and skin color in an
880 admixed population via Bayesian linear mixed models. *Genetics* **206**, 1113–1126 (2017).

881 [64] Kemper, K. E., Bowman, P. J., Hayes, B. J., Visscher, P. M. & Goddard, M. E. A multi-
882 trait Bayesian method for mapping QTL and genomic prediction. *Genetics Selection
883 Evolution* **50**, 10 (2018).

884 [65] Marquez-Luna, C. *et al.* Modeling functional enrichment improves polygenic predic-
885 tion accuracy in UK biobank and 23andMe data sets. *bioRxiv* 375337 (2018).

886 [66] Gazal, S. *et al.* Linkage disequilibrium–dependent architecture of human complex
887 traits shows action of negative selection. *Nature Genetics* **49**, 1421 (2017).

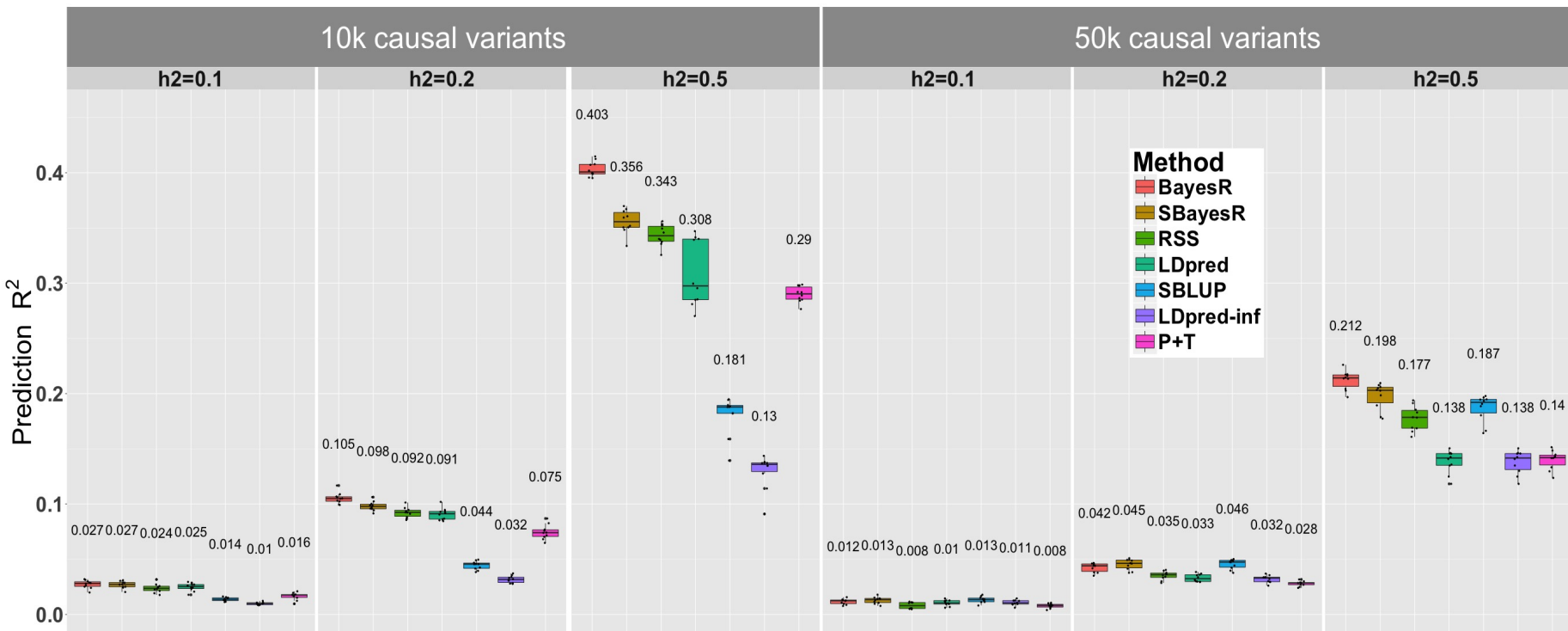


Figure 1 Prediction accuracy performance for the UKB genome-wide simulation. Each panel displays boxplot summaries of the prediction R^2 (y-axis) in the 10,000 individual validation data set for each method (x-axis) across the 10 replicates. The simulation study contained six scenarios that varied in the number of causal variants, 10,000 (10k) and 50,000 (50k), and the true simulated heritability $h_{SNP}^2 = (0.1, 0.2, 0.5)$. The two genetic architecture scenarios generated were: 10,000 causal variants sampled under the SBayesR model i.e., 2500, 5000, and 2500 variants from each of $N(0, 0.01)$, $N(0, 0.1)$, and $N(0, 1)$ distributions respectively, and 50,000 causal variants sampled from a standard normal distribution. For each replicate a new sample of causal variants was chosen at random from the set of 1,094,841 HapMap 3 variants. In each panel LDpred has two boxplot summaries, one that has been optimised for the polygenicity parameter and the other is LDpred-inf, which is displayed for comparison with SBLUP. The mean prediction accuracy across the 10 replicates is displayed above the boxplot for each method.

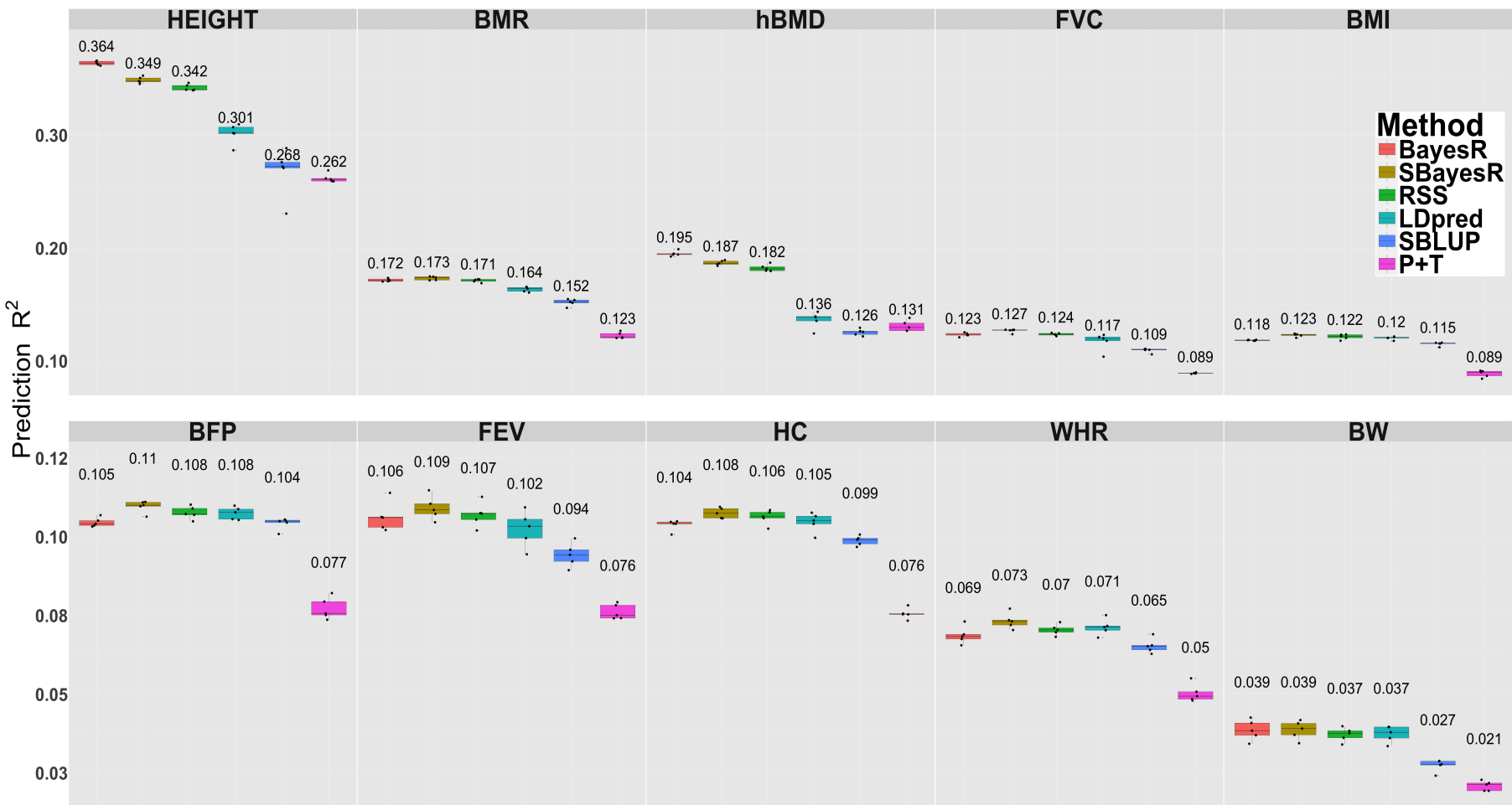


Figure 2 Prediction accuracy in five-fold cross-validation for 10 quantitative traits in the UK Biobank. Panel headings describe the abbreviation for 10 quantitative traits including: standing height (HEIGHT, $n=347,106$), basal metabolic rate (BMR, $n=341,819$), heel bone mineral density T-score (hBMD, $n=197,789$), forced vital capacity (FVC, $n=317,502$), body mass index (BMI, $n=346,738$), body fat percentage (BFP, $n=341,633$), forced expiratory volume in one-second (FEV, $n=317,502$), hip circumference (HC, $n=347,231$), waist-to-hip ratio (WHR, $n=347,198$) and birth weight (BW, $n=197,778$). Each panel shows a boxplot summary of the prediction R^2 across the five folds with the mean across the five folds displayed above each method's boxplot. Traits are ordered by mean estimated h_{SNP}^2 (see Figure S14) from highest to lowest.

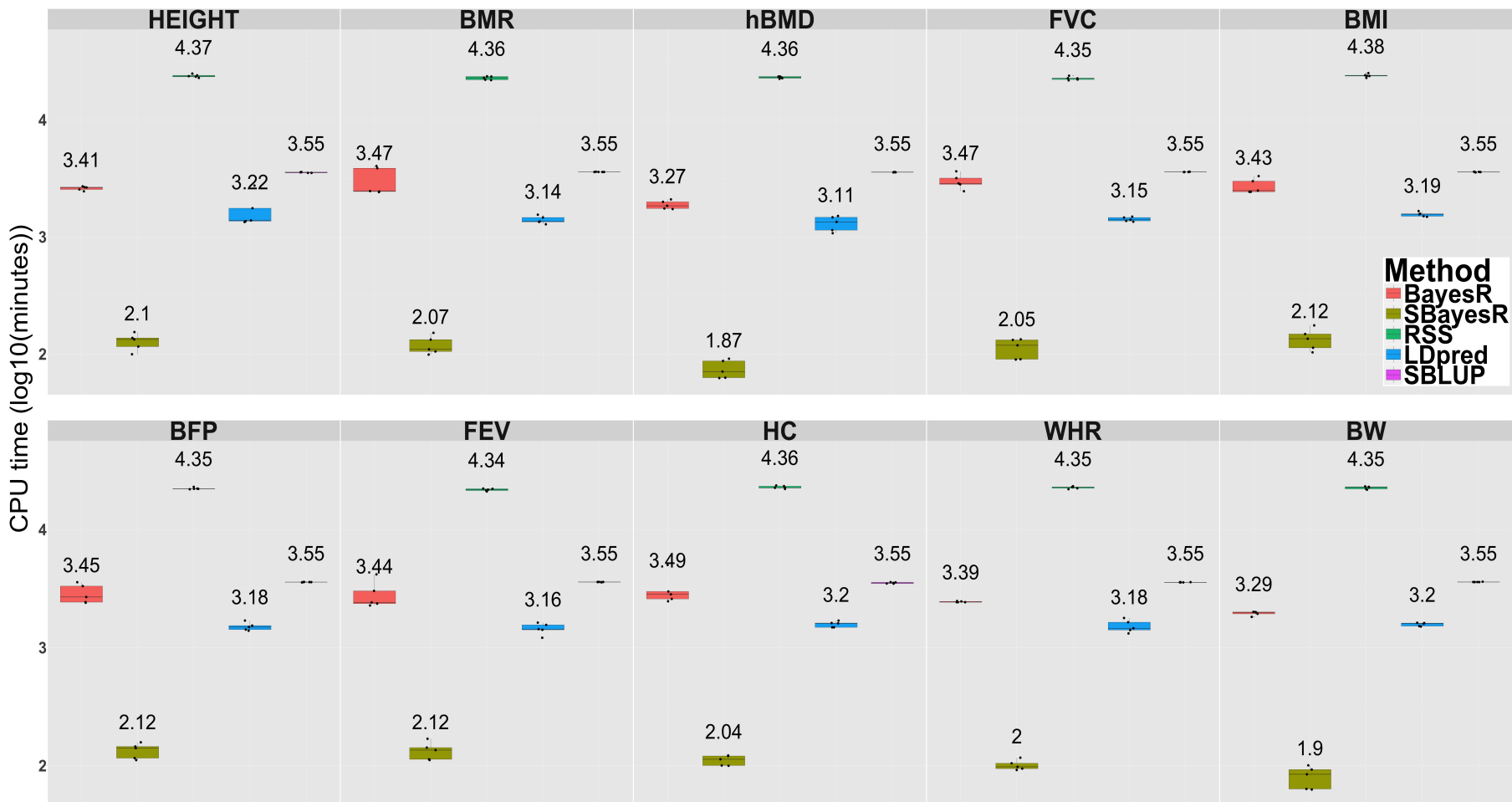


Figure 3 Runtime ($\log_{10}(\text{minutes})$) comparison for BayesR, SBayesR, RSS, LDpred and SBLUP in cross-validation analysis of 10 quantitative traits in the UKB. Panel headings describe the abbreviation for 10 quantitative traits including: standing height (HEIGHT, $n=347,106$), basal metabolic rate (BMR, $n=341,819$), heel bone mineral density T-score (hBMD, $n=197,789$), forced vital capacity (FVC, $n=317,502$), body mass index (BMI, $n=346,738$), body fat percentage (BFP, $n=341,633$), forced expiratory volume in one-second (FEV, $n=317,502$), hip circumference (HC, $n=347,231$), waist-to-hip ratio (WHR, $n=347,198$) and birth weight (BW, $n=197,778$). Each panel shows a boxplot summary of runtime with the mean across the five folds displayed above each method's boxplot. Results for RSS, LDpred and SBLUP represent the sum over time for each chromosome-wise analysis. Results for RSS and SBayesR do not include the time to compute the LD reference matrix. Results for P+T, HEreg and LDSC are not shown as they required relatively minimal computing resources.

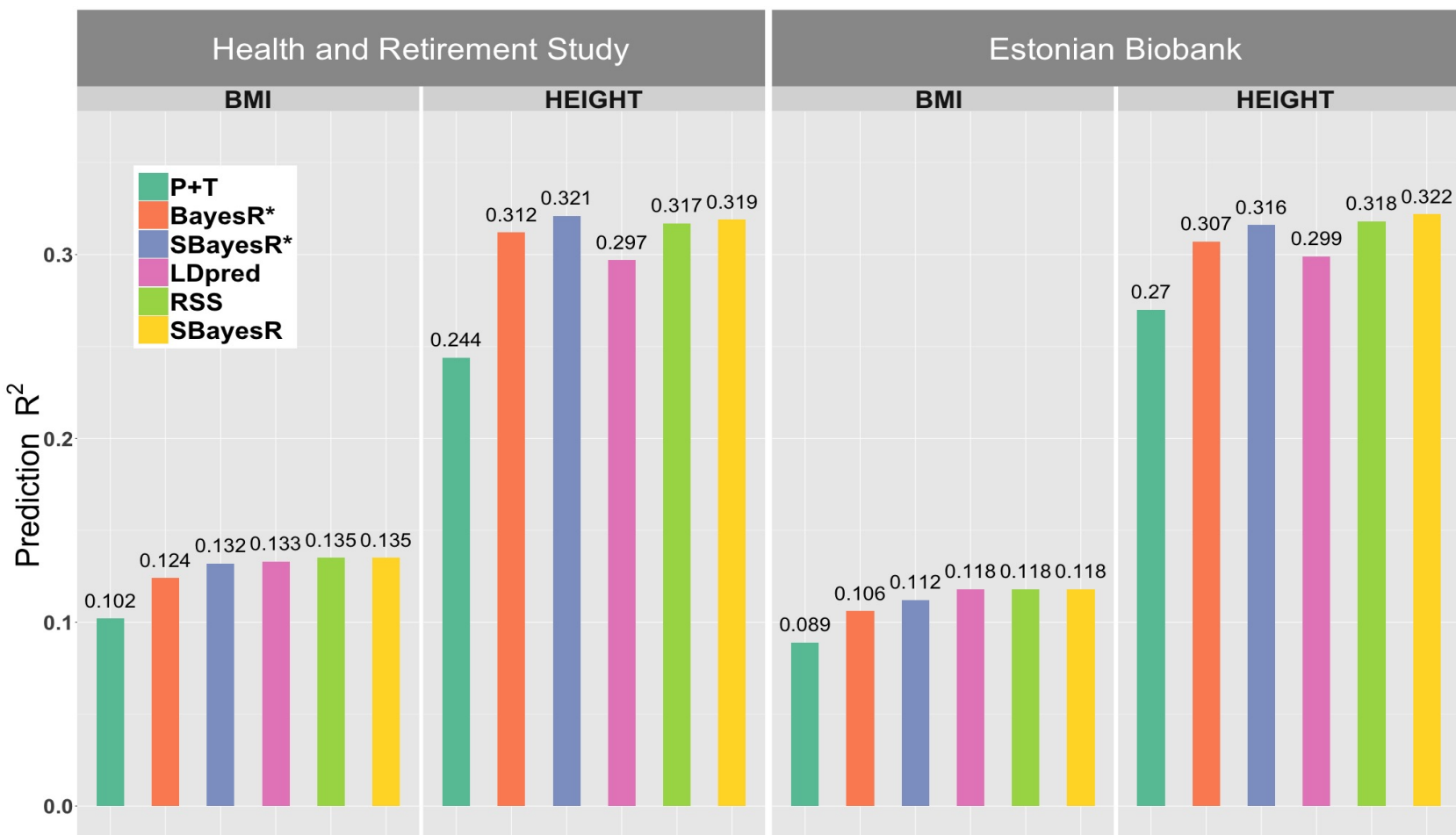


Figure 4 Prediction accuracy for height and body mass index in the independent Health and Retirement Study and Estonian Biobank data sets. Panels depict prediction R^2 (y-axis) generated from regression of the predicted phenotype on the observed phenotype for body mass index (BMI) and height for different methods in the independent HRS and ESTB data sets. P+T refers to the prediction R^2 generated from the summary statistics of Yengo *et al.* 2018 ($n \approx 700,000$), which included 6,781 SNPs for BMI and 11,816 SNPs for height from a GCTA-COJO analysis thresholded at p -value < 0.001 . The BayesR* and SBayesR* predictions were calculated using 1,094,841 HM3 variants estimated from the full set of unrelated and related UKB European individuals ($n = 453,458$ and $n = 454,047$ for BMI and height respectively). Summary statistics for SBayesR analysis for the UKB European individuals were generated using the BOLT-LMM software. All other prediction R^2 results were generated using summary statistics methodology and were calculated from the analysis of summary statistics from Yengo *et al.*⁴⁹ for 909,293 and 932,969 variants for BMI and height that overlapped with the 1,094,841 HM3 variants set used for the UKB analyses. The overlap of the sets of variants used in each of the analyses and those available in the imputed HRS and ESTB data sets for prediction had a minimum value of 98%.